Consistency of Fanbeam Projections Along an Arc of a Circle

Rolf Clackdoyle, Michel Defrise, Laurent Desbat, and Johan Nuyts

***Abstract*-- New data consistency conditions (DCCs) are presented for fanbeam projections taken along an arc of a circle. They are found by performing a weighted backprojection onto a line segment; consistency is manifested as polynomial behavior along the line. An application to a toy problem illustrates the behavior and potential of these DCCs.**

I. Introduction

Data consistency conditions (DCCs) have had a role in image reconstruction for many years. The idea is that the projection data are redundant, and these redundancies, which are specified using DCCs, have been exploited to tease out unwanted physical effects in the imaging system. The many examples in the literature suggest that DCC applications can be successfully achieved if the physical effects are modelled with a small handful of suitable parameters. Natterer [Nat93a] was probably the first to follow this paradigm when he used DCCs for attenuated SPECT data to estimate the best affine transformation of a prototype attenuation map. "Best" means that the estimated affine transformation, when applied to the measurements, yielded the most consistent data. There have been dozens of other examples of DCC applications in PET, SPECT, and CT.

In this work, we are only concerned with consistency conditions for single-slice (2D) reconstruction using the attenuation-free model, suitable for x-ray CT.

An essential component for DCC applications is a mathematical description of the DCCs themselves. The well-known Helgason-Ludwig (H-L) conditions [Lud66, Hel80] apply to unattenuated parallel projections, and have the notable advantages that (i) they are *full* (both necessary and sufficient), and (ii) they can be applied to any subset of (untruncated) parallel projections. In contrast to this situation is the case of fanbeam projections on a circular trajectory. The standard approach for fanbeam projections has been to reformulate them (either mathematically, or by rebinning the data) into parallel projections, and then applying the H-L conditions. This approach has the disadvantage that only a tomographically complete set, such as a full 2π scan or at least a standard shortscan, can be tested for consistency[1] (e.g. [Fin83a, Pat02, Yu06]). Other DCCs for circular fanbeam projections that don't make use of the parallel H-L conditions can be found [Lou89, Nat93b, Maz10] but these also all require a complete set of fanbeam projections on the circle.

For fanbeam projections with source positions along a straight line rather than on a circle, DCCs have recently been established [Cla13] that are similar in flavor to the H-L conditions: they are full, and they can be applied to any subset of (untruncated) fanbeam projections. Similar DCC results for fanbeam projections on a circle seem to be more difficult to obtain, but the straight-line case can be leveraged to achieve partial results. For example, any two source locations on a circular trajectory can be considered to lie on a "virtual" straight line trajectory connecting the two sources, so the straight-line DCCs can be applied. For just two projections however, there can be no conditions higher than order zero, and these order zero conditions, which can be applied for any two (untruncated) fanbeam projections, have been known for some time [Fin83b, Noo02, Che05, Wei06, Lev10] (see also the discussions in [Tan12] and [Cla13]). For a small finite number of projections on the circle, the projections can only be checked pairwise using these conditions (see [Wei06, Cla14] for some example applications), and higher-order conditions would be stronger. (Order zero conditions cannot detect inconsistencies due to certain motions of the object, for example.)

In this work, the straight-line conditions are leveraged in a different way, to allow any (reasonably) small arc of the circular trajectory to be tested for consistency for any order (not just order zero). The idea is to consider the chord that connects the endpoints of the arc, and to rebin the true fanbeam projections onto virtual fanbeam projections with virtual sources along the chord. The virtual fanbeam projections will also be untruncated and the mapping is one-to-one, so the conditions on the arc will be full if and only if the conditions on the chord are full. However, due to the rebinning, the whole arc must be simultane-

R. Clackdoyle is with the Laboratoire Hubert Curien, CNRS UMR 5516, Saint Etienne, France (e-mail: rolf.clackdoyle@univ-st-etienne.fr).

M. Defrise is with the Dept. of Nuclear Medicine, Vrije Universiteit Brussel, B-1090, Brussels, Belgium (e-mail: mdefrise@vub.ac.be).

L. Desbat is with the TIMC-IMAG laboratory, CNRS UMR 5525, and Joseph Fourier University, Grenoble, France (e-mail: laurent.desbat@imag.fr).

J. Nuyts is with KU Leuven - University of Leuven, Department of Imaging and Pathology, Nuclear Medicine & Molecular imaging, Medical Imaging Research Center, B-3000 Leuven Belgium (email: johan.nuyts@uzleuven.be).

This work was partially supported by the Agence Nationale de la Recherche (France), project "DROITE," number ANR-12-BS01-0018; and partially supported by the SRP10 program of the Vrije Universiteit Brussel.

[1]Note: the principle of rebinning circular fanbeam projections into parallel projections can be also applied to incomplete fanbeam trajectories. If the length of the fanbeam trajectory segment is larger than the FOV, then rebinning into a small angular range of parallel projections is possible, and the H-L conditions can be applied. However, only a small fraction of the fanbeam rays contribute to the rebinning and are tested for consistency.

ously checked (or else subdivided into small chords). The restriction on the length of the arc is that the chord must not cut the field-of-view (FOV) where the support of the object is assumed to lie. The rebinning is performed mathematically so that closed form expressions are obtained for the fanbeam-arc DCCs.

We present these new DCCs below, and provide a numerical demonstration, including a model application with a highly artificial toy problem.

II. Theory

We denote fanbeam projection data by $g(\lambda, \gamma)$ where the source position is indicated by the angular parameter λ, which is measured counterclockwise from the vertical. The ray direction is parametrized by angle γ, measured relative to the source. The unknown 2D density function is $f(x, y)$.

$$g(\lambda, \gamma) = Tf(\lambda, \gamma) = \int_0^\infty f(\bar{s}_\lambda + l\hat{n}_{\lambda,\gamma})dl \qquad (1)$$

The source location is given by $\bar{s}_\lambda = (-R\sin\lambda, R\cos\lambda)$, and the integration direction by $\hat{n}_{\lambda,\gamma} = (\sin(\lambda+\gamma), -\cos(\lambda+\gamma))$. See Figure 1 (left).

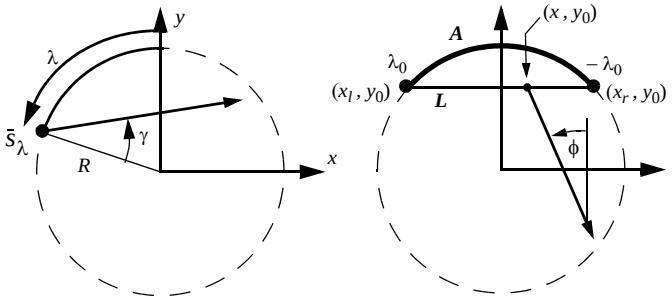

Figure 1. Left: Illustration of the fanbeam variables λ indicating the source position, and γ for the ray. Right: The arc A and its chord L are shown. A virtual fanbeam vertex is at (x, y_0) with ray direction ϕ.

We now consider any arc A of the circle, provided it is not too long (see below). Without loss of generality, we can consider the arc to be of length $2\lambda_0$, starting at $\lambda = -\lambda_0$ and ending at $\lambda = \lambda_0$, as illustrated in Figure 1 (right). We are looking for DCCs for the projections whose sources lie along A. We let L represent the chord joining the endpoints of the arc A, and label these endpoints as (x_l, y_0) and (x_r, y_0). See Figure 1 (right).

We define the virtual fanbeam projection $g_v(x, \phi)$ whose virtual source is located at $(x, y_0) \in L$, and whose ray direction is given by ϕ measured counterclockwise from the vertical as shown in Figure 1 (right).

$$g_v(x, \phi) = T_v f(x, \phi) = \int_0^\infty f((x, y_0) + l(\sin\phi, -\cos\phi))dl \quad (2)$$

For each $n = 0, 1, 2\ldots$, and for $x \in [x_l, x_r]$, we define the weighted sum of the virtual projection rays for the source at (x, y_0) by

$$B_n(x) = \int_{-\pi/2}^{\pi/2} g_v(x, \phi)\frac{\tan^n\phi}{\cos\phi}d\phi \qquad (3)$$

Now if the support of f does not intersect the line $y = y_0$, then $g_v(x, \phi) = 0$ for $|\phi|$ near $\pi/2$, and therefore the powers of $\cos\phi$ in the denominator of the integrand of (3) do not cause difficulty. Under this condition on the support of f, necessary DCCs for the virtual fanbeam projections are easily obtained [Cla13]:

If a given function g_v satisfies $g_v = T_v f$ for some f, then for all $n = 0, 1, 2, \ldots$, the function $B_n(x)$ is a polynomial in x of degree (at most) n.

DCCs for the projections g on the arc A can be obtained by re-expressing equation (3) for $B_n(x)$ with a similar expression using $g(\lambda, \gamma)$ instead of $g_v(x, \phi)$. This is the mathematical equivalent of "rebinning to virtual fanbeam projections". Fixing x and considering Figure 2, the ray in the direction ϕ from virtual source location (x, y_0) can be found from the source position $(-R\sin\lambda, R\cos\lambda)$ as shown, and we obtain

$$\tan\phi = \frac{x + R\sin\lambda}{R\cos\lambda - y_0} \qquad (4)$$

and thus $g(\lambda, \gamma) = g_v(x, \phi)$ where γ $(= \phi - \lambda)$ can be found using equation (4) resulting in

$$\cos\gamma = \frac{R + x\sin\lambda - y_0\cos\lambda}{D_{x,\lambda}} \qquad (5)$$

with $D_{x,\lambda} = \left\|(-R\sin\lambda, R\cos\lambda) - (x, y_0)\right\|$ being the distance between the λ-source and the virtual source at (x, y_0). Taking the derivative of equation (4) to obtain the Jacobian, the right-hand-side of equation (3) can now be converted to projections on the arc, to obtain our main result:

$$B_n(x) = \int_{-\lambda_0}^{\lambda_0} g(\lambda, \gamma)W_n(x, \lambda)d\lambda \qquad (6)$$

$$W_n(x, \lambda) = \frac{(R\sin\lambda + x)^n}{(R\cos\lambda - y_0)^{n+1}}(R\cos\gamma) \qquad (7)$$

If a given fanbeam function g along an arc satisfies $g = Tf$ for some f, then for all $n = 0, 1, 2, \ldots$, the function $B_n(x)$ given by equations (6) and (7) is a polynomial in x of degree (at most) n.

Note that the arc should be short enough that the chord does not intersect the FOV of the scanner, to ensure the support condition on f for the virtual fanbeam DCCs.

One notable difference between the arc projections and the

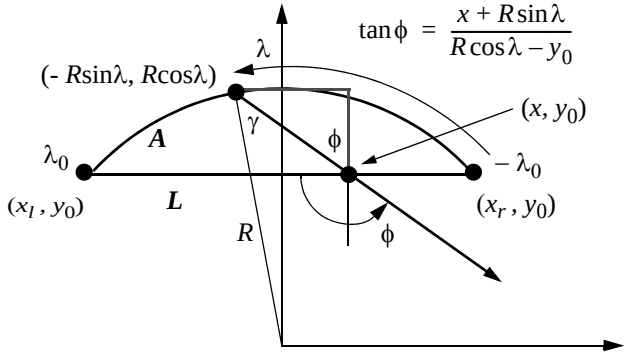

Figure 2. Rebinning to the virtual fanbeam projection. The relationship between ϕ and λ (both measured from the vertical) is illustrated, for a fixed virtual fanbeam source point (x, y_0). The arrows indicate the pivoting of the ray about the virtual source point during integration.

virtual projections is that the integration takes place over the ray variable ϕ for the virtual projections, whereas the integral is over the source index on the arc. Equation (6) can be interpreted and implemented as a weighted backprojection of the fanbeam projections onto the line segment L. The weight is given by equation (7). A linear interpolation is needed for the γ variable (the ray variable).

The arc projections $g(\lambda, \gamma)$ should not be truncated.

III Simulations

A. Illustration of DCCs on an arc

For all the simulation studies shown, the fanbeam source radius R was 140 mm with a FOV radius of 100 mm. The arc was 60^o in total length, so $\lambda_0 = \pi/6$. The tight radius of the fanbeam trajectory was chosen to emphasize the fanbeam character of this work. For this choice of R and λ_0, the segment L lies on the line $y = y_0$ with $y_0 = 70\sqrt{3} \approx 121.2$ which is outside the FOV as shown in Figure 3. Details of the mathematical phantom are also shown in Figure 3.

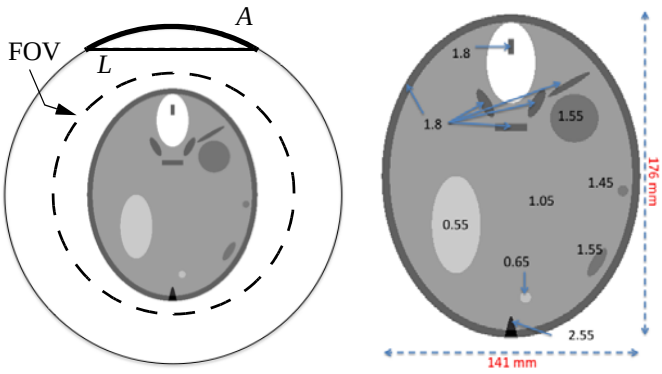

Figure 3. Left: a scale diagram of the geometry used for the simulations. The FOV radius is 100 mm, the 60^o arc lies on the trajectory of radius 140 mm, so the line segment is at $y = 121.2$. Right: intensity details of the phantom.

Figure 4 illustrates the full 360^o trajectory of fanbeam projections (1024 rays per projection) simulated analytically from the elliptical phantom. A standard FBP reconstruction is also shown. For the rest of this work, only the 340 projections covering the first 60^o of arc were processed.

From the 340 fanbeam projections (in increments of 0.176^o) along the arc A, a backprojection implementation was

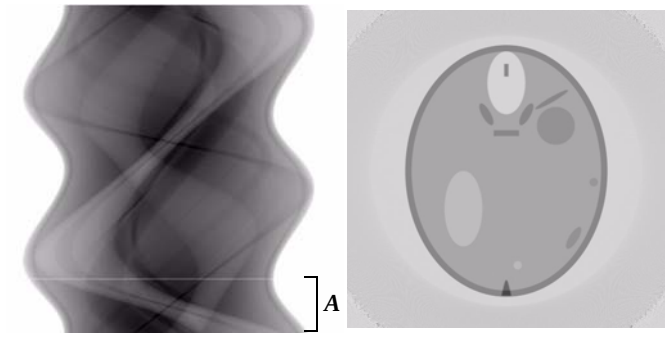

Figure 4. Left: the full 360^o of fanbeam projections simulated mathematically from the elliptical phantom. The bottom line is $\lambda = -30^o$ and white line indicates $\lambda = 30^o$. Right: standard reconstruction from full fanbeam data.

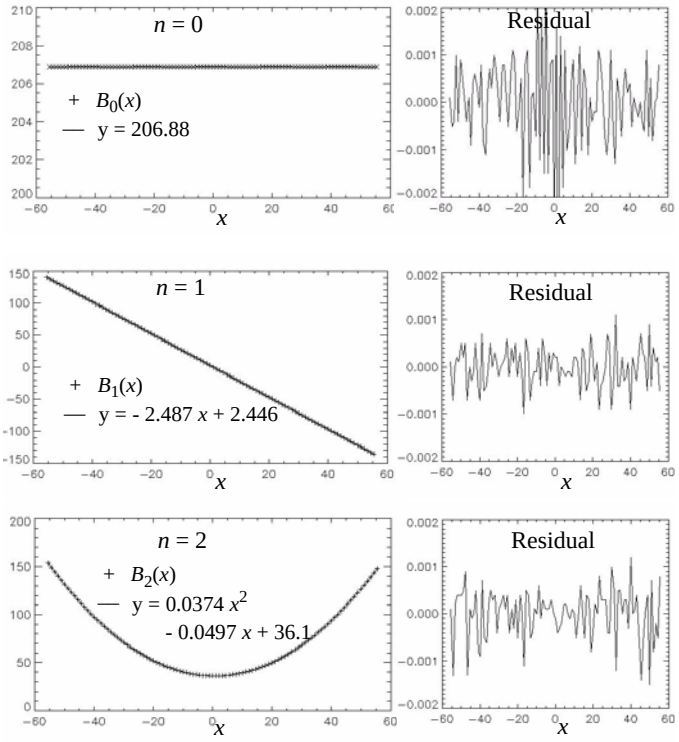

Figure 5. Left: plots of the calculated $B_n(x)$ functions sampled at 101 values of x, with the best-fit degree n polynomial superimposed. Right: plots of the residuals, the difference between $B_n(x)$ and its best polynomial.

used to compute $B_n(x)$ given by equation (6), for 101 equally spaced values of x ranging from -55.4 to +55.4 in steps of 1.1 mm along the line segment L and for each of $n = 0, 1, 2$. Using standard least squares techniques, polynomials of degree n were fit to $B_n(x)$ and superimposed in the plots shown in Figure 5. The residuals (differences between $B_n(x)$ and the best degree-n polynomial) were also plotted.

The results show that $B_n(x)$ follows the predicted polynomial behavior very closely. The residuals were unstructured and at roughly the level of machine precision errors (single precision).

B. An example DCC application using a toy problem

For our toy problem, we imagine that the detector gain reduces exponentially during the $2\lambda_0$ segment of the scan along the arc. ("The detector gets tired.") The actual measured projections g_m are related to g by

$$g_m(\lambda, \gamma) = g(\lambda, \gamma)e^{-\tau\lambda} \qquad (8)$$

according to an unknown exponential constant τ (per radian).

The 60^o of fanbeam projections from section III.A above were multiplied by exponential factors according to equation (8) to provide measured projections with unknown τ (known only to the co-author who simulated the projections), with roughly a 20% intensity reduction at the end of the 60^o arc. A second sinogram was also formed by then adding about 10% Poisson noise to each measurement. Figure 6 shows the image of the projections and a plot at the central ray location of each projection. The noisy sinogram is readily discernible, but

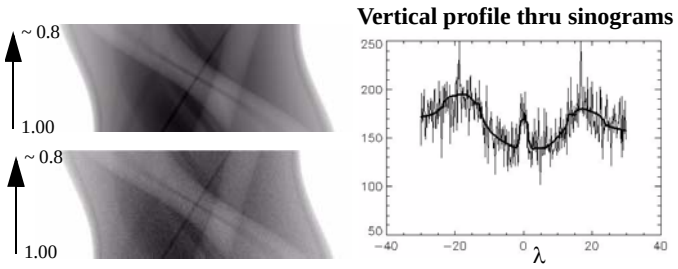

Figure 6. Fanbeam projection data for the toy problem. Upper left: the simulated data include an exponential decay with increasing angle λ resulting in about 80% intensity at $\lambda = +30^{o}$. Lower left: the same sinogram with roughly 10% Poisson noise included. Right: superimposed plots at the central ray location ($\gamma = 0$) through the two sinograms. The exponential effect is barely discernible.

the exponential factors are difficult to ascertain.

When checking the DCCs with the noise-free exponentially weighted projections we found, as expected, poor agreement with the polynomials. Although Figure 7 suggests good polynomial behavior for $n = 1, 2$, we observe that the residuals are highly structured, and are four orders of magnitude larger than for the ideal projections of section III.A. These observations inspired the following procedure to estimate the unknown τ.

A cost function was defined as the sum of the three square residuals (the three "mean-square differences" with their best-fit polynomials). Trial estimates $\tilde{\tau}$ were checked by first multiplying $g_m(\lambda, \gamma)$ by $e^{\tilde{\tau}\lambda}$ and then checking the cost function

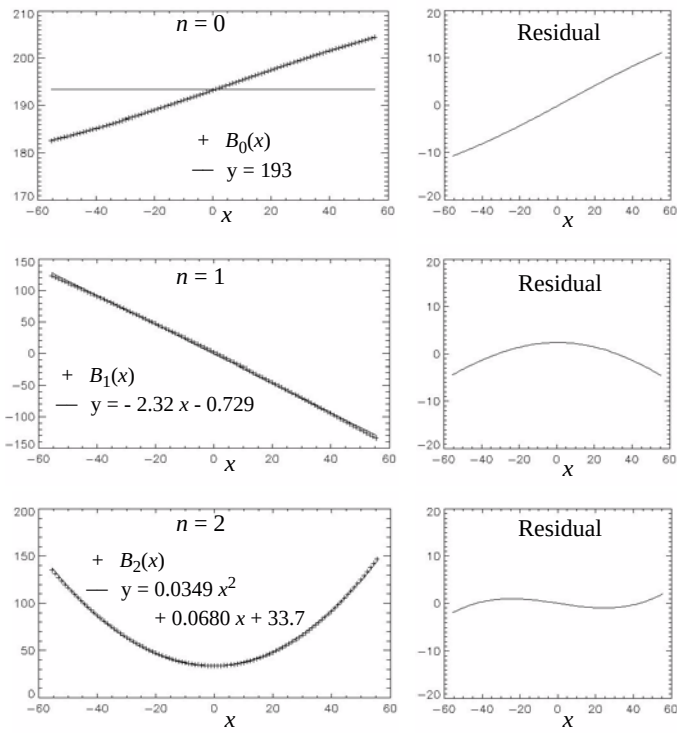

Figure 7. Similar to figure 5, for $n = 0, 1\ 2$, the exponentially-modified (noise-free) fanbeam projections were backprojected to form $\overline{B_n}(x)$ which were plotted along with their best fit polynomial. The residuals are plotted on the right. This time the residuals are highly structured, and 10,000 times larger than before (compare vertical scales with Figure 5).

using the resulting backprojections $B_n^{\tilde{\tau}}(x)$. The golden-section search method [Vet02] was applied to find the best τ^* that minimized the cost function. Thus when the DCCs were satisfied, we deemed the detector to be correctly compensated by $e^{\tau^*\lambda}$. The experiment was performed for both the noisy and the noiseless projection data.

For the noisy data, the golden-section search converged after 35 iterations to $\tau^* = -0.130064$ from the initial values of $\tau_{\text{left}} = -1.0$, $\tau_{\text{right}} = 1.0$. Further study of the cost function revealed highly non-convex behavior (many local minima) very close to τ^* (within about 0.000001), so we would cautiously suggest $\tau^* = -0.13006$, and for greater confidence we would estimate $\tau^* = -0.1301$. The cost function had a minimum value of 1.2

For the noise-free data, the golden-section search revealed that the cost function had a minimum value of 0.0000014 at $\tau^* = -0.130144$ (although it might be reasonable to justify a single-precision result of $\tau^* = -0.1301439$ considering the small leading digit.)

The optimization searches were performed "blind" and only after the above results were established was the true exponential value revealed. It was $\tau_{\text{true}} = -0.130145$.[2]

IV. Discussion and Conclusions

We have outlined the derivation of new DCCs for fanbeam projections along an arc. The arc must be short enough that its chord does not intersect the scanner field-of-view.

The principle behind these new DCCs is a mathematical rebinning to virtual fanbeam projections along the chord, from which known DCCs were applied. This same technique was recently applied in DCC theory for *truncated* fanbeam projections along a *complete* trajectory [Cla15]. Despite the significantly different geometries, many of the same equations appear since the essential circle-to-chord rebinning step is the same.

The results of our simulation experiments suggested that the DCCs are not particularly sensitive to zero-mean noise, but are highly sensitive to systematic effects on the projections, such as a small exponential weighting. The DCC method easily identified the exponential factor to multiple-digit accuracy.

V. References

[Cla13]R. Clackdoyle. "Necessary and Sufficient Consistency Conditions for Fanbeam Projections along a Line." *IEEE Trans Nucl Sci* 60, 1560-1569, 2013.

[Cla14]R. Clackdoyle, S. Rit, J. Hoskovec, L. Desbat. "Fanbeam Data Consistency Conditions for Applications to Motion Detection" *The Third International Meeting on Image Formation in X-Ray Computed Tomography, Salt Lake City, USA. June 22-25, 2014*. Pages: 324-328.

[Cla15]R. Clackdoyle and L. Desbat. "Data consistency conditions for truncated fanbeam and parallel projections." *Med Phys* 42, (in press) 2015.

[Che05]G.-H. Chen and S. Leng. "A new data consistency condition for fan-beam projection data." *Med Phys* 32, 961-967, 2005.

[Fin83a]D.V. Finch and D.C. Solmon. "A characterization of the range of the divergent beam X-ray transform." *SIAM J Math*

[2]The choice of τ (130145) used in the simulations was to honour the main organiser (DWT) of the first "Fully 3D" Meeting in 1991, on the occasion of his 70th birthday in January of this year.

Anal 14, 767–771, 1983.

[Fin83b]D.V. Finch and D.C. Solmon. “Sums of homogeneous function and the range of the divergent beam X-ray transform.” *Numer Func Anal and Optimiz* 5, 363–419, 1983.

[Hel80]S. Helgason. *The Radon Transform.* (Boston: Birkhauser), 1980.

[Lev10]M.S. Levine, E.Y. Sidky and X. Pan. “Consistency Conditions for Cone-Beam CT Data Acquired with a Straight-Line Source Trajectory.” *Tsinghua Sci Technol* 15, 56–61, 2010.

[Lou89]A K. Louis and A. Rieder. “Incomplete Data Problems in X-Ray Computerized Tomography II. Truncated Projections and Region-of-Interest Tomography.” *Numer. Math.* 56, 371–383, 1989.

[Lud66]D. Ludwig. “The Radon transform on Euclidean space.” *Comm. Pure Appl. Math.* 19, 49–81, 1966.

[Maz10]S.R. Mazin and N.J. Pelc. “Fourier properties of the fanbeam sinogram.” *Med. Phys* 37, 1674-1680, 2010.

[Nat93a]F. Natterer. “Determination of tissue attenuation in emission tomography of optically dense media.” *Inv. Probs* 9, 731–736, 1993.

[Nat93b]F. Natterer. “Sampling in fan beam tomography.” *SIAM J Appl Math* 53, 358-380, 1993.

[Noo02]F. Noo, M. Defrise, R. Clackdoyle, H. Kudo. “Image reconstruction from fan-beam projections on less than a short-scan.” *Phys. Med. Biol.* 47, 2525-2546, 2002.

[Pat02] S.K. Patch. “Consistency conditions upon 3D CT data and the wave equation.” *Phys. Med. Biol*. 47, 2637-2650, 2002.

[Tan12]S. Tang, Q. Xu, X. Mou, and X. Tang, “The mathematical equivalence of consistency conditions in the divergent-beam computed tomography,”*J. X-Ray Sci. Tech.*, 20, 45–68, 2012

[Vet02]W. Vetterling, S.A. Teukolski, W.H. Press, B.P. Flannery. *Numerical Recipes. Example Book (C++)* second edition. (Cambridge University Press), 2002.

[Wei06]Y.Wei, H.Yu, and G.Wang, “Integral invariants for computed tomography,”IEEE Signal Process. Lett. 13, 549–552 (2006).

[Yu06] H. Yu, Y. Wei, J. Hsieh and G. Wang. “Data Consistency Based Translational Motion Artifact Reduction in Fan-Beam CT.” *IEEE Trans. Med. Imag.* 25, 792–803, 2006.